

## **Nuclear Transmutation in Actinoid Hydrides and Deuterides**

Hideo Kozima

Cold Fusion Research Laboratory

597-16, Yatsu, Aoi, Shizuoka, 421-1202 Japan

### **Abstract**

Nuclear transmutations observed in the cold fusion phenomenon (CFP) have attracted attention from various points of view. Our sense of wonder at events in the CFP is based on the common sense that phenomena occurring in a nucleus are isolated from the drama played in the world of atoms outside of the nucleus without few exceptional cases such as the Knight shift in NMR, the change of K-capture probability by environment and the Moessbauer effect where they show weak connections between two world.

As have been revealed by many experimental data sets observed in the CFP, there are various events showing occurrence of nuclear reactions in materials composed of host elements and hydrogen isotopes (protium or/and deuterium) with a comparable ratio to the host (cf-materials) even when there is no specific acceleration mechanism. In the events of nuclear reactions observed in the CFP, one of the most interesting is the nuclear transmutations of nuclei with several decay channels (including radioactive nuclei such as  $^{235}_{92}\text{U}$  and  $^{231}_{90}\text{Th}$ ) in free space. To explain these transmutations it was necessary to assume a gigantic shortening of the decay time in cf-materials compared to that observed in free space.

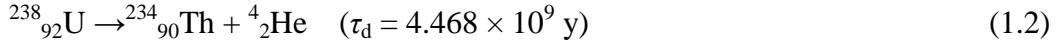
We have proposed a model (TNCF model) to give a successful unified explanation for various events in the CFP from excess energy generation, emissions of charged particles and neutron, and to nuclear transmutations. The experimental data sets on the nuclear transmutation of radioactive nuclei obtained in the CFP include many details of the measurements and give us materials for their analysis if we can use them properly. In this paper, we used the knowledge of nuclear physics on the interaction of a nucleus and neutron sea (corresponding to the cf-matter in our model) to give a unified and consistent explanation of the decay-time shortening observed in uranium (and thorium) hydrides and deuterides prepared by the implantation in a glow discharge or by the absorption in electrolyses.

### **1. Introduction – Spontaneous and Induced Decay of Actinoids**

In the history of nuclear physics, we have noticed the existence of nuclei which decay spontaneously. The actinoids are the typical nuclides which show this characteristic. They also show induced decays absorbing a neutron. These characteristics are written down as reaction formulae as follows;

### 1.1 Spontaneous disintegrations

(1) Spontaneous Alpha Decay of Actinoids – Examples with half-lives  $\tau_d$  in parentheses.

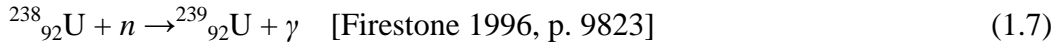
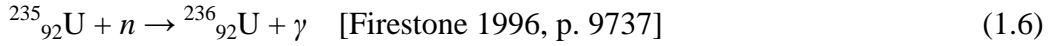


(2) Spontaneous fission – Examples



### 1.2 Nuclear transmutations induced by neutron absorption

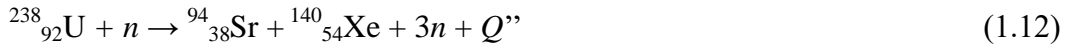
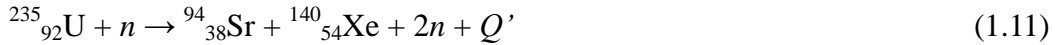
(1) Gamma emission after absorption of a neutron – Examples



(2) Alpha decay induced by neutron absorption – Examples



(3) Fission induced by neutron absorption - Examples



We have proposed a model (TNCF model) to give a successful unified explanation for various events in the cold fusion phenomenon (CFP) from excess energy generation, emissions of charged particles and neutron, and to nuclear transmutations investigated after 1989. It is a characteristic of the CFP that it has been observed only in specific solids (cf-materials) composed of lattice nuclei and hydrogen isotopes with comparable number densities to each other.

The original assumption of the existence of the “trapped neutron” in the TNCF model proposed in 1993 [Kozima 1994] has been replaced by formation of a new state (cf-matter) composed of quasi-free neutrons and a little protons and electrons to neutralize it as a whole in the recent quantal investigation of premises of the TNCF model [Kozima 2006 (Sec. 3.7.5), 2008c].

In the investigation of the nuclear reactions of actinoids in cf-materials, we have to consider nuclear reactions induced by spontaneous mechanisms as listed above in 1.1

and also those induced by absorption of neutrons as listed in 1.2. Furthermore, as we have discussed several times (cf. [Kozima 2006, 2014b]), it is necessary to consider not only reactions induced by absorption of a neutron (as in 1.2) but also those induced by absorption of a nucleon cluster  ${}^A_Z\Delta$  composed of  $Z$  protons and  $(A - Z)$  neutrons. In this paper, however, we confine our investigation only assuming the cases induced by the absorption of a single neutron for simplicity.

Then, we have to investigate the disintegrations of actinoid nuclei in their hydrides and deuterides as observed in the experiments as shown in Section 2 taking possible reactions (1.1) – (1.12) into our consideration as discussed in Section 3.

## 2. Experimental Data Sets of CFP in Actinoids Hydrides and Deuterides

There are several works on the emission of neutrons and charged particles in actinoid hydrides and deuterides. In this section, we introduce several data sets from the works performed in the history of the CF research to investigate them from our point of view in the next section.

### 2.1 Neutron Emission in $\text{UD}_3$ and $\text{TiD}_x$

Neutron emissions in uranium deuteride ( $\text{UD}_3$ ) and deuterium-loaded titanium ( $\text{TiD}_x$ ) samples were measured with a detector of high detection efficiency [Jiang 2012]. The efficiency of detection was calibrated by  ${}^{252}\text{Cf}$  neutron source to be greater than 50%.

The “cascade bursts” of neutrons were measured several times only for  $\text{UD}_3$  and  $\text{TiD}_x$  ( $x = 1$  and  $1.4$ ) samples but not for control samples of uranium oxide and deuterium-unloaded Ti foils. The authors suggested that the cascade neutron bursts might originate in the nuclear reactions occurring in the surface region of samples with widths of a micro-nanometer size.

This result suggests that the neutron emission in both  $\text{UD}_3$  and  $\text{TiD}_x$  may be induced by the same cause. We have proposed a mechanism where the cf-matter is responsible for nuclear reactions in the CFP based on the TNCF model [Kozima 2011a]. The suggestion of surface nature of the emission of neutrons by Jiang et al. is consistent with our explanation of neutron-nuclear interactions in localized regions at surface where the cf-matter is apt to be formed [Kozima 2011b].

Uranium nucleus fissions spontaneously into two nuclei and a neutron (or neutrons). The observation of neutrons emitted from  $\text{UD}_3$  and  $\text{TiD}_x$  by Jiang et al. suggests that the emission of neutrons in uranium deuteride is fundamentally governed by the CFP in cf-materials. So, we may be able to investigate the emission of charged particles in

actinoid hydrides and deuterides using our model which has been successfully applied to various events in the CFP.

## 2.2 Radiations of Actinoid Hydrides and Deuterides

J. Dash and his collaborators in Portland State University, Oregon, USA have extensively studied characteristic changes of the decay patterns of uranium and thorium in their compounds with protium (hydrogen) and deuterium [Goddard 2000, Dash 2003a, 2003b, 2005]. The compounds were prepared by the methods using electrolysis and glow discharge.

In the case of glow discharge [Dash 2003a, 2003b], they confirmed using gamma ray spectroscopy that there are thorium isotopes identified as  $^{231}_{90}\text{Th}$  and  $^{234}_{90}\text{Th}$  which are expected to be generated from  $^{235}_{92}\text{U}$  and  $^{238}_{92}\text{U}$  by alpha decays (1.1) and (1.2), respectively. This is a typical example of the “decay-time shortening” for the reactions by the formation of cf-matter as discussed in other papers presented at this Conference [Kozima 2014a (Sec. 2.10), 2014b (Sec. 6.5.3)]. The decay-time shortening, i.e. a drastic decrease of the decay constant of an unstable nucleus in cf-materials from that in free space, of alpha disintegration is expected when there is formed the neutron star matter (or cf-matter in the case of the CFP) surrounding the quasi-stable nuclei which disintegrates by alpha emission.

However, there remains some ambiguity if the gamma spectra used to determine the thorium isotopes are not identified as due to  $^{231}_{90}\text{Th}$  and  $^{234}_{90}\text{Th}$ . If they are due to  $^{232}_{90}\text{Th}$  and  $^{235}_{90}\text{Th}$ , the observed spectra are consistent with the mechanism of alpha decay after single neutron absorption of  $^{238}_{92}\text{U}$  and  $^{235}_{92}\text{U}$ , respectively.



Therefore, we have to be cautious to investigate changes of the decay characteristic of actinoids in cf-materials which depend various variables in the sample.

### 2.2.1 Co-deposition of $\text{U}_3\text{O}_8$ and H on Ni Cathode with Acidic Electrolyte and Pt Anode

Co-deposition of  $\text{U}_3\text{O}_8$  and H on Ni cathodes with an acidic electrolyte and a Pt anode was performed [Goddard 2000]. In this case, they measured increase of the radiation from 2900 (control) to 3700 counts (co-deposited sample) measured by a G-M counter for the same amount of  $\text{U}_3\text{O}_8$ . There are observed existence of Cs, Fe and Ni on the nickel cathode and also topography change of the surface in the form of donut-like eruptions as shown in Fig. 2.1.

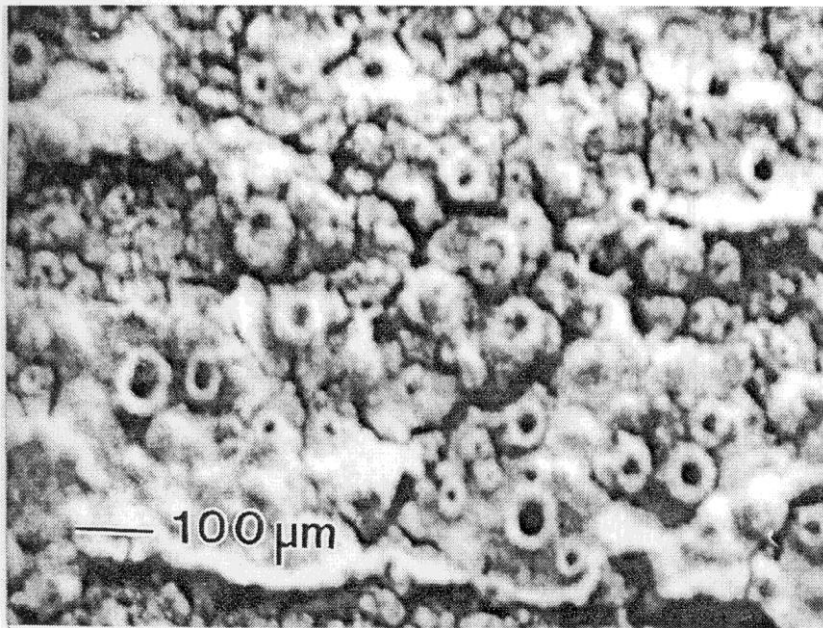


Fig. 2.1. Typical micrograph of U<sub>3</sub>O<sub>8</sub> electroplated on a nickel cathode after experiment.

### **Radiation**

The radiation emitted by the electroplated U<sub>3</sub>O<sub>8</sub> (A) was compared with radiation emitted by unelectrolyzed U<sub>3</sub>O<sub>8</sub> (B).

(A) Initially produced about 2900 counts/3 minutes (4-17-00). This increased sporadically in steps to ~ 3700 counts/(3 minutes) (5-11-00) and stayed there until 6-8-00 when ended the measurements.

(B) Emitted ~ 1250 counts/(3 minutes) remaining almost constant over the entire period of measurements.

### **Gamma spectroscopy**

The net integral of 86 peaks of measured  $\gamma$ -radiation from a 10 mg sample in 25 hours gave 53,000 counts (A) and 31,000 counts (B).

### **Surface topography**

Observation by a SEM (scanning electron microscope) showed that Donut-like features appeared showing voids surrounded by raised circular rims (Fig. 2.1).

### **New elements**

Cesium (Cs), iron (Fe) and nickel (Ni) (and possibly fermium (Fm)) are detected by EDS (energy dispersive spectrometer).

## **2.2.2 Implantation of Hydrogen Isotopes into Uranium Cathode by Glow Discharge**

Uranium foils were attached to the cathode made of stainless steel in a glow discharge apparatus. Either hydrogen or deuterium ions was implanted to uranium by the glow discharge at a voltage of about 500 V [Dash 2003a].

There are four samples exposed to plasmas; 1) H1 (to H<sub>2</sub> plasma for 43 hours), 2) H2 (to H<sub>2</sub> plasma for 18 hours), 3) D1 (D<sub>2</sub> plasma for 100 hours), 4) D2 (D<sub>2</sub> plasma for 500 hours).

Alpha, beta and gamma measurements were made on samples exposed to the plasmas and compared with the results on a control uranium foil without exposure. An example of measurements is shown in Fig. 2.2 for the gamma radiation measured on August and November of 2001 and April of 2002 [Dash 2003a (Fig. 4)]. Here, we notice a positive correlation between the implantation time and the intensity of the gamma radiation of uranium.

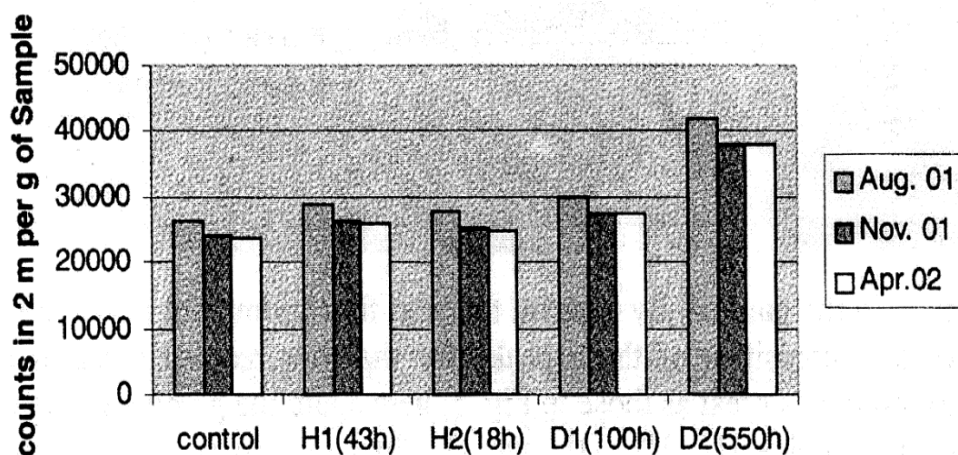


Fig. 2.2. Gamma radiation from uranium samples after exposure to hydrogen isotope plasmas [Dash 2003a].

Samples were examined with a SEM and analyzed with an EDS.

1) **Approximate counts of alpha-, beta- and gamma-radiations per gram of uranium** (after [Dash 2003a, Figs. 2, 3 and 4]).

Table 2.1. Counts of alpha-, beta- and gamma radiations per gram of uranium after exposure to hydrogen isotope plasmas.

	Control	H1	H2	D1	D2
$\alpha$ (in 2 hours $\times 10^{-4}$ )	2.3	6.0	5.9	6.0	11.4
$\beta$ (in 2 min. $\times 10^{-5}$ )	1.70	1.85	1.80	1.95	2.75
$\gamma$ (in 2 min. $\times 10^{-4}$ )	2.50	2.67	2.55	2.72	3.92

In this table, we notice the strong correlation of the increases of the  $\alpha$ -,  $\beta$ - and  $\gamma$ -radiations and the implantation times of deuterium D<sub>2</sub> in D1 and D2 samples.

**2) Approximate net counts of 98.5 keV characteristic X-ray of  $^{238}_{92}\text{U}$  per gram of sample** (after [Dash 2003a, Fig. 6])

Table 2.2. Counts of 98.5 keV characteristic X-ray of  $^{238}_{92}\text{U}$  per gram of sample after exposure to hydrogen isotope plasmas.

	Control	H1	H2	D1	D2
X (in 24 hours $\times 10^{-4}$ )	3.1	2.9	3.1	2.75	2.2

**3) Approximate net counts of 92.4 keV characteristic gamma ray of  $^{234}_{90}\text{Th}$  per gram of sample** (after [Dash 2003a, Fig. 5])

Table 2.3. Counts of 92.4 keV characteristic X-ray of  $^{234}_{90}\text{Th}$  per gram of sample after exposure to hydrogen isotope plasmas.

	Control	H1	H2	D1	D2
$\gamma$ (in 2 min. $\times 10^{-4}$ )	1.90	2.30	2.35	2.60	2.75

Decrease of  $^{238}_{92}\text{U}$  in Table 2.2 and increase of  $^{234}_{90}\text{Th}$  in Table 2.3 corresponding to the implantation time may be explained by the reaction (1.2).

**4) Approximate net counts of 186 keV characteristic gamma ray of  $^{235}_{92}\text{U}$  per gram of sample** (after [Dash 2003a, Fig. 7])

Table 2.4. Counts of 186 keV characteristic gamma ray of  $^{235}_{92}\text{U}$  per gram of sample after exposure to hydrogen isotope plasmas.

	Control	H1	H2	D1	D2
$\gamma$ (in 24 hours $\times 10^{-4}$ )	3.74	3.86	3.86	3.86	4.14

Increase of  $^{235}_{92}\text{U}$  corresponding to the implantation time in D1 and D2 samples will

be discussed in Sec. 3.3.1.

The confirmation of  $^{234}_{90}\text{Th}$  [Dash 2003a] seems credible and the reaction (1.2) is reliable for the case of glow discharge experiment and the decay-time shortening is induced by the mechanism in terms of the cf-matter as discussed in our papers [Kozima 2014a, 2014b].

The surface topography observed by SEM showed pit structure after the electrolysis as shown in Fig. 2.3.

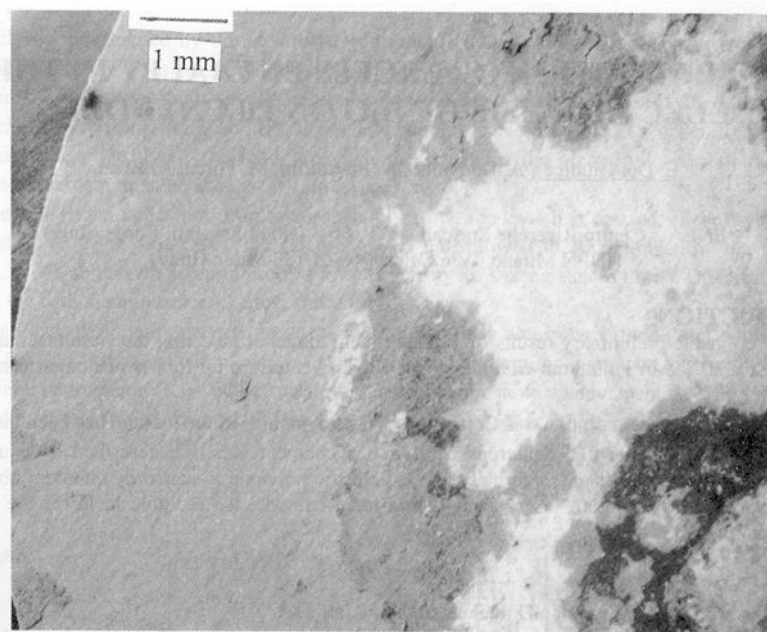


Fig. 2.3. SEM photograph of uranium sample D2 after exposure to deuterium plasma for about 550 hours. The relatively smooth rim on the left was protected from exposure to the plasma by a molybdenum nut which fastened the sample against the cathode.

### 2.2.3 Hydrogen Loading of Uranium by Electrolysis

Natural uranium foil of 0.18 mm thick and purity 99.98% was used as a cathode in electrolysis with 0.83 M and 0.74 M  $\text{H}_2\text{SO}_4$  electrolyte in  $\text{H}_2\text{O}$  [Dash 2005]. Anode was platinum plate. The alpha, beta and gamma specific radioactivity were measured after the hydrogen loading and compared with the control. Gamma ray spectroscopy was also performed by EDS on the samples.

For two series of experiments, they obtained similar results to that obtained in discharge experiments (cf. Sec. 2.2.2): increases of  $^{234}_{90}\text{Th}$  and  $^{235}_{92}\text{U}$  characteristic gamma spectra and decrease of  $\text{K}_{\alpha 1}$  characteristic X-ray peak of  $^{238}_{92}\text{U}$ .

The surface concentration (within a depth of about 1  $\mu\text{m}$ ) was determined by EDS.

Increase of thorium and decrease of carbon was observed. The former is consistent with the spectroscopic measurement given above. The decrease of carbon in the surface region is not explained at present.

### **3. Analysis of Experimental Data Sets**

The cold fusion phenomenon (CFP) has been observed in solids composed of host elements and hydrogen isotopes with almost equal number densities of both components (cf-materials). Typical examples of the cf-materials are PdD<sub>x</sub> ( $x = 0.75 \sim 1.0$ ), NiH<sub>x</sub> ( $x \sim 1.0$ ), TiD<sub>x</sub> ( $x \sim 2.0$ ), (CH<sub>x</sub>)<sub>n</sub> (XLPE,  $x \sim 2.0$  and  $n = \infty$ ). Using a model (TNCF model) based on the experimental data, we have been able to explain semi-quantitatively various features of the CFP from production of excess energy to nuclear transmutations through emissions of charged particles and neutron [Kozima 2006, 2008a, 2010a, 2010b]. The investigation of the basis of the TNCF model has shown possible formation of a specific state of neutrons (cf-matter) in cf-materials having a characteristic super-lattice made of interlaced sublattices of host elements and hydrogen isotopes [Kozima 2006 (Sec. 3.7.3), 2008c].

The experimental data of Jiang et al. [Jiang 2012] introduced above has given us a fact that the neutron emission of uranium deuteride has a common characteristic of the CFP. Therefore, we may investigate the CFP in the actinoid hydrides and deuterides from our point of view which have been used successfully for the analyses of the CFP in other cf-materials.

#### **3.1 Mechanism of the Cold Fusion Phenomenon (CFP) suggested by the TNCF Model**

The nuclear reactions generating various events in the CFP occur in solids composed of host elements and hydrogen isotopes with comparable number densities of both components (cf-materials) at near room temperature (at most several hundred degrees Kelvin). To answer the natural question how to overcome the Coulomb barrier between charged particles against nuclear reactions, we have assumed existence of “trapped neutrons” in cf-materials. The model based on this fundamental premise (TNCF model) has given unified explanation of whole events in the CFP suggesting the existence of a hidden clue in the premises of the model.

The investigation of the premise of the trapped neutron has been elaborated using knowledge of transition metal hydrides in solid state physics and of exotic nuclei in nuclear physics [Kozima 2006]. The fundamental idea to show possible existence of “trapped neutrons” in cf-materials is the neutron bands generated by neutrons in lattice

nuclei of host elements mediated by interstitial protons (or deuterons) in the cf-materials. The neutrons in a band formed by this mechanism constitute a “quasi-free neutron gas” (cf-matter) and interact with foreign nuclei in the lattice or with dislocated nuclei of the host element especially in surface region and also in volume [Kozima 2012]. This situation is schematically depicted in Fig. 3.1.

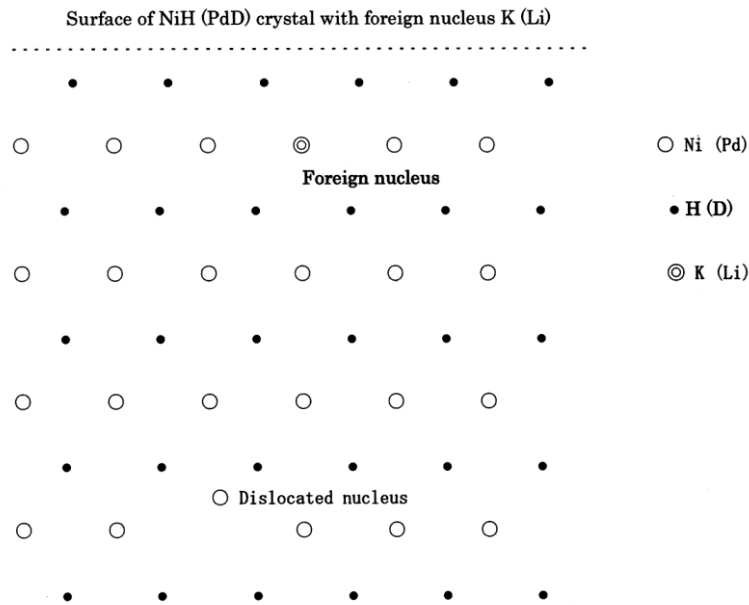


Fig. 3.1. Schematic 2-dimensional picture of the host lattice nuclei Ni (Pd), the interstitial hydrogen isotope H (D) and the foreign nucleus K (Li) in a NiH (PdD) crystal.

The experimental data obtained by Jiang et al. [Jiang 2012] has shown that the neutron emissions in  $UD_3$  and in  $TiD_x$  have similarity. This fact suggests us that the cf-matters responsible to the CFP have been formed similarly in both cf-materials. A regular super-lattice is formed at least locally which is made of a sublattice of uranium (U) and another sublattice of deuteron (D) interlacing each other. The lattice structures of uranium deuterides  $UD_3$  are given in the next subsection.

### 3.2 Structure of Uranium Hydride

Uranium hydrides and deuterides have been investigated as a neutron moderator, a nuclear fuel for the nuclear pile, and a bank of hydrogen storage.

The lattice of uranium hydride expands considerably during formation and  $UH_3$  is therefore not an interstitial compound. In its lattice, each uranium atom is surrounded by

6 other uranium atoms and 12 atoms of hydrogen; each hydrogen atom occupies a large tetrahedral hole in the lattice. The density of hydrogen in uranium hydride is approximately the same as that in liquid water or in liquid hydrogen. The U-H-U linkage through a hydrogen atom is present in the structure [Rundle 1947]. This linkage reminds us the super-nuclear interaction of lattice nuclei (e.g. Pd) mediated by the interstitial hydrogen isotopes (e.g. D) in transition-metal hydrides and deuterides (e.g. PdD) depicted similarly as Pd-D-Pd linkage [Kozima 2006, Fig. 3.3].

There exist two crystal modifications of uranium hydride. They are both cubic: an  $\alpha$  form that is obtained at low temperatures and a  $\beta$  form that is grown when the formation temperature is above 250 °C. After growth, both forms are metastable at room temperature and below, but the  $\alpha$  form slowly converts to the  $\beta$  form upon heating to 100 °C. Both  $\alpha$ - and  $\beta$ -UH<sub>3</sub> are [ferromagnetic](#) at temperatures below ~180 K. Above 180 degrees K, they are paramagnetic [Wikipedia, *Uranium hydrides*].

The lattice structures of the  $\alpha$  and the  $\beta$  forms of UH<sub>3</sub> compounds are shown in Figs. 3.2 and 3.3, respectively [Katz 1986].

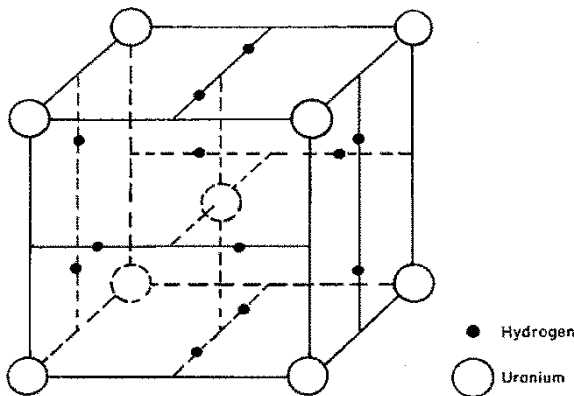


Fig. 3.2. Lattice structure of  $\alpha$ -UH<sub>3</sub> [Katz 1986].

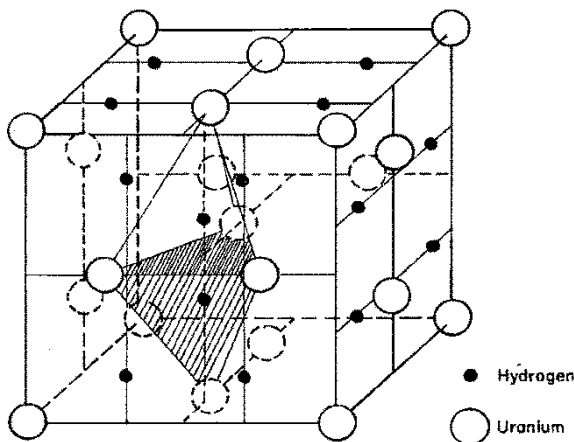


Fig. 3.3. Lattice structure of  $\beta$ -UH<sub>3</sub> [Katz 1986].

The structures of  $\text{UH}_3$  shown in Figs. 3.2 and 3.3 demonstrate the complex feature of the  $\text{UH}_3$  structure compared with other cf-materials such as  $\text{PdD}_x$ ,  $\text{NiH}_x$  and XLPE. However, how the structure of the  $\text{UH}_3$  is complex, the regularity of the arrays of uranium and hydrogen in each sublattices suffices the condition for formation of neutron bands speculated in our papers to legitimate the existence of cf-matter [Kozima 2006, 2008c].

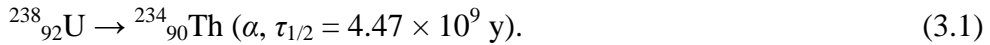
Therefore, we may be able to apply our model to the experimental data sets of nuclear transmutations in actinoid hydrides and deuterides introduced in Section 2.

### 3.3 Explanation of Experimental Data Sets introduced in Section 2 and Decay-Time Shortening by TNCF Model

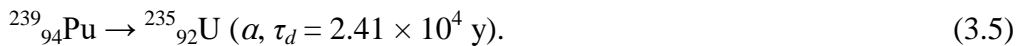
The experimental data sets obtained by Goddard et al. [Goddard 2000] and Dash et al. [Dash 2003, 2005] revealed a common characteristic of decay-time shortening of actinoid hydrides and deuterides irrelevant to their methods of formation. The positive correlation between implantation time of hydrogen isotopes into uranium and amounts of radiation (by the decay-time shortening) (cf. Fig. 2.2) is interpreted as an indication that the formation of cf-matter in the sample is provided by the formation of the superlattice of uranium and hydrogen isotopes from our point of view (cf. Sec. 3.3.2).

#### 3.3.1 Explanation of Nuclear Transmutation observed in Experiments

The decrease of  $^{238}_{92}\text{U}$  and increase of  $^{235}_{92}\text{U}$  and  $^{234}_{90}\text{Th}$  observed by Dash et al. (cf. Sec. 2.2.3) is explained by following reactions. The increase of  $^{234}_{90}\text{Th}$  is due to the decay-time shortening of the following spontaneous decay process (Eq. (1.2)) with a decay time  $\tau_d$  of  $4.468 \times 10^9$  year in free space:



The increase of  $^{235}_{92}\text{U}$  may be the successive reactions (decay type, half-life in free space) started from the reaction (1.7) followed by  $\beta$ -decays and an  $\alpha$ -decay of resultant nuclides written down as follows:



Again, the decay reaction (3.5) may be accelerated by the decay-time shortening in the cf-material.

The rise of radiation observed in the experiment by Goddard et al. (cf. Sec. 2.2.1) is

explained by the increase of the decay reaction (3.1) by the decay-time shortening. The appearance of Fe and Cs on the cathode and the morphology change of the cathode surface have shown the occurrence of nuclear transmutations accompanying excess heat in this system but without data on its mechanism.

The increases of  $^{234}_{90}\text{Th}$  and  $^{235}_{92}\text{U}$  determined by characteristic gamma rays in the experiment by Dash et al. (cf. Sec. 2.2.2) are also indication of the nuclear reactions written down in Eqs. (3.1) – (3.5). The morphology change of the surface shown in Fig. 2.3 clearly shows the occurrence of nuclear reactions accompanying a huge excess heat generation resulting in the nuclear transmutation described by these equations even if there is no observation of the transmuted nuclei  $^{239}_{92}\text{U}$ ,  $^{239}_{93}\text{Np}$  and  $^{239}_{94}\text{Pu}$ .

### 3.3.2 Explanation of the Decay-time Shortening

As has been shown in our papers presented at this conference [Kozima 2014a, 2014b], the height of the surface layer of radioactive nucleus preventing emission of nucleons in free space becomes lower according to the increase of the density  $n_o$  of neutrons in free space becomes lower according to the increase of the density  $n_o$  of neutrons in the cf-matter surrounding the nucleus with a neutron density  $n_i$ , or the increase of the density ratio  $n_o/n_i$  of neutrons outside and inside the nucleus. This feature is depicted in Fig. 3.4 where the surface energy of the boundary  $E_{\text{surf}} (\equiv y)$  decreases with the increase of the density ratio  $n_o/n_i (\equiv x)$  [Negele 1973].

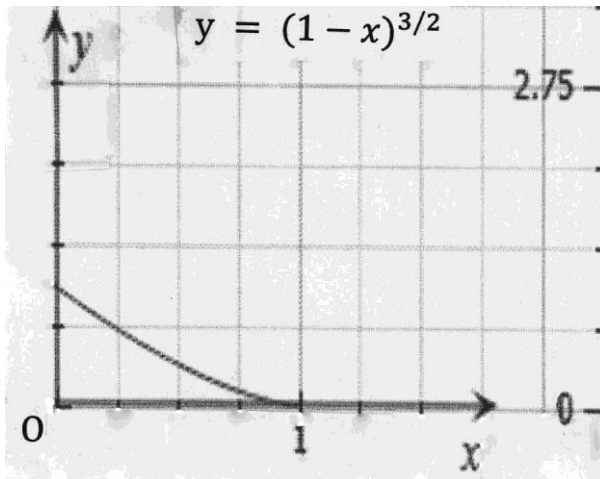


Fig. 3.4. Dependence of the surface energy  $E_{\text{surf}} (\equiv y)$  on the density ratio  $n_o/n_i (\equiv x)$ .

It is clear that the lower the surface energy of the boundary, the easier a nucleon escapes from the nucleus. The same logic will be applicable to the emission of an alpha particle from a nucleus to explain the decay-time shortening observed by Dash et al.

[Goddard 2000, Dash 2003, 2005] by the formation of a high-density neutron medium (cf-matter) in the cf-material, especially at its surface or boundary region [Kozima 2006, 2014a].

Instability of the metastable states of  $UD_3$  (transition from  $\alpha$  to  $\beta$ -phase explained in Sec. 3.2) shows that it is difficult to realize a stable superlattice of  $UD_3$  ( $UH_3$ ) composed of a uranium sublattice and a deuteron (proton) sublattice. This may be the reason that there is a temporal change of radiation for samples irradiated by plasmas (e.g. Fig. 2.2)

It is reasonable that the amount of increase in  $\alpha$ -radiation has positive correlation to the average density of hydrogen isotopes which is surely proportional to the time of plasma discharge and electrolysis (e.g. Table 2.1).

Thus, the data sets of the decay-time shortening of uranium and thorium introduced above are consistently explained by the TNCF model using the concept of cf-matter suggested by the neutron star matter elaborated in 1970's in relation to the explanation of the neutron star [Baym 1971, Negele 1973].

## 4 Conclusions

Experimental data sets on actinoid hydrides and deuterides have been analyzed and explained using the TNCF model. The experimental data have shown that these hydrides and deuterides are classified as the cf-materials where occurs the cold fusion phenomenon (CFP) and the observed events are understood by nuclear reactions common to other reactions observed in cf-materials, mainly transition-metal hydrides and deuterides.

The changes of radiation properties of actinoids occluding hydrogen isotopes are explained by formation of the cf-matter similar to the free neutron sea in neutron star matter and then by the interaction of actinoid nucleus and the cf-matter. Acceleration of the alpha decay of  $^{238}_{92}\text{U}$  into  $^{234}_{90}\text{Th}$ , the so-called the decay-time shortening, is explained by the change of the boundary layer between the nucleus  $^{238}_{92}\text{U}$  and the cf-matter induced by the increase of the density ratio  $n_o/n_i$  of neutrons due to the formation of the cf-matter.

A possible application of this phenomenon to  $^A_{94}\text{Pu}$  ( $A = 238 - 244$ ) is hopeful.

If we can handle plutonium isotopes which are produced in atomic plants as hazardous waste properly to accelerate their decay, it is the savior of our age from the dangerous nuclear waste waiting its resolution. As shown in Table 4.1, plutonium isotopes have very long decay times and therefore the decay-time shortening as shown

in the CFP will be applicable to transmute them into other nuclides easy to treat with.

Table 4.1 Decay characteristics of plutonium isotopes

Isotope	Decay mode	Half-life	Decay heat	Spon. fission neutrons
$^{238}_{94}\text{Pu}$	alpha to $^{234}_{92}\text{U}$	87.74 (y)	560 (W/kg)	2600 (1/g • sec)
$^{239}_{94}\text{Pu}$	alpha to $^{235}_{92}\text{U}$	24100	1.9	0.022
$^{240}_{94}\text{Pu}$	alpha to $^{236}_{92}\text{U}$	6560	6.8	910
	+ Spont. Fission			
$^{241}_{94}\text{Pu}$	$e^-$ to $^{241}_{95}\text{Am}$	14.4	4.2	0.049
$^{242}_{94}\text{Pu}$	alpha to $^{238}_{92}\text{U}$	376000	0.1	1700

Instead of neutron bombardment in free space, we can use the cf-materials to give an effect of neutrons on target nuclei. This fact may be interesting in science and technology of the neutron-nuclear interaction in low energy region.

### Acknowledgement

The author would like to express his thanks to Prof. John Dash of Portland State University for valuable discussions during this work and also to Dr. S.-S. Jiang of China Institute of Atomic Energy for his kindness to send him the paper published in *Chin. Phys. Lett.* He is also indebted to Prof. H. Sukanuma of Shizuoka University for his help in obtaining information about structures of  $\text{UH}_3$  and valuable discussions with him.

### References

- [Baym 1971] G. Baym, H.A. Bethe and C.J. Pethick, "Neutron Star Matter," *Nuclear Physics*, A175, 225 – 271 (1971).
- [Dash 1993] J. Dash, G. Noble and D. Diman, "Surface Morphology and Microcomposition of Palladium Cathodes after Electrolysis in Acidified Light and Heavy Water: Correlation with Excess Heat," *Trans. Fusion Technol.*, 26, 299 – 306 (1993).
- [Dash 1994a] J. Dash, G. Noble and D. Diman, "Changes in Surface Topography and Microcomposition of a Palladium Cathode caused by Electrolysis in Acidified Light Water," *Proc. Int. Sym. Cold Fusion and Advanced Energy Sources* (Minsk, Belarus, May 25 – 26, 1994) pp. 172 – 183 (1994).
- [Dash 1994b] J. Dash, G. Noble and D. Diman, "Surface Morphology and Microcomposition of Palladium Cathodes after Electrolysis in Acidified Light and Heavy Water: Correlation with Excess Heat," *Proc. ICCF4*, 2, pp. 25-1 – 25-11 (1994).

- [Dash 1996] J. Dash, "Chemical Changes and Excess Heat caused by Electrolysis with  $\text{H}_2\text{SO}_4 - \text{D}_2\text{O}$  Electrolyte," *Proc. ICCF6*, pp. 477 – 481 (1996).
- [Dash 1997] J. Dash, R. Kopecek and S. Miguet, "Excess Heat and Unexpected Elements from Aqueous Electrolysis with Titanium and Palladium Cathodes," *Proc. 32th Intersociety Energy Conversion Engineering Conference*, 2, pp. 1350 – 1355 (1997).
- [Dash 2003a] J. Dash, I. Savvatimova, S. Frantz, E. Weis and H. Kozima, "Effects of Glow Discharge with Hydrogen Isotope Plasmas on Radioactivity of Uranium," *Proc. ICCF9*, pp.77 – 81 (2003). ISBN 7-302-06489-X/O·292
- [Dash 2003b] J. Dash, H. Kozima, I. Savvatimova, S. Frantz and E. Weis, "Effects of Glow Discharge with Hydrogen Isotope Plasmas on Radioactivity of Uranium," *Proc. 11th Intern. Conf. Emerging Nuclear Energy Systems*, p.122 – 126 (2003).
- [Dash 2005] J. Dash and D. Chicea, "Changes in the Radioactivity, Topography, and Surface Composition of Uranium after Hydrogen Loading by Aqueous Electrolysis," *Proc. ICCF10* pp. 463 – 474 (2005). ISBN 981-256-564-7
- [Firestone 1996] R.B. Firestone, *Table of Isotopes*, CD-ROM 8<sup>th</sup> edition, v. 1.0, Wiley-Interscience, 1996.
- [Fleischmann 1989] M. Fleischmann, S. Pons and M. Hawkins, "Electrochemically induced Nuclear Fusion of Deuterium," *J. Electroanal. Chem.*, 261, 301 – 308 (1989).
- [Goddard 2000] G. Goddard, J. Dash and S. Frantz, "Characterization of Uranium Codeposited with Hydrogen on Nickel Cathodes," *Transactions of American Nuclear Soc.* **83**, 376 – 378 (2000).
- [Jiang 2012] S. Jiang, X. Xu et al., "Anomalous Neutron Burst Emissions in Deuterium-Loaded Metals: Nuclear Reaction at Normal Temperature," *Chinese Physics Lett.*, **29**, pp. 112501-1 – 4 (2012). And also S. Jiang, X. Xu et al., "Neutron Burst Emission from Uranium Deuteride and Deuterium-Loaded Titanium," *Proc. ICCF17* (preprint version).
- [Katz 1986] J.J. Katz, G.T. Seaborg and L.R. Morss, *The Chemistry of the Actinide Elements*, Vol.1 (Second Edition), Chapman and Hall, 1986.
- [Kozima 1994] H. Kozima, "Trapped Neutron Catalyzed Fusion of deuterons and Protons in Inhomogeneous Solids," *Trans. Fusion Technol.*, **26**, 508 – 515 (1994). ISSN 0748-1896.
- [Kozima 1998] H. Kozima, *Discovery of the Cold Fusion Phenomenon* (Ohtake Shuppan Inc., 1998). ISBN 4-87186-044-2.
- [Kozima 2002] H. Kozima, "An Explanation of Data Sets obtained by McKubre et al. (Excess Heat), Clarke (Null Results of  $^4\text{He}$  and  $^3\text{He}$ ) and Clarke et al. (Tritium) with

‘Arata Cell,’” *Proc. ICCF9*, pp. 182 – 185 (2002). ISBN 7-302-06489-X/O ·292

[Kozima 2006] H. Kozima, *The Science of the Cold Fusion Phenomenon*, Elsevier Science, 2006. ISBN-10: 0-08-045110-1.

[Kozima 2008a] H. Kozima, “Phenomenology of the Cold Fusion Phenomenon,” *Reports of CFRL (Cold Fusion Research Laboratory)*, **8-3**, pp. 1 – 23 (September, 2008).  
<http://www.geocities.jp/hjrfq930/Papers/paperr/paperr.html>

[Kozima 2008b] H. Kozima, W.W. Zhang and J. Dash, “Precision Measurement of Excess Energy in Electrolytic System Pd/D/H<sub>2</sub>SO<sub>4</sub> and Inverse-Power Distribution of Energy Pulses vs. Excess Energy,” *Proc. ICCF13*, pp. 348 – 358 (2008). ISBN 978-5-93271-428-7. And also *Reports of CFRL* **11-5**, pp. 1 – 14 (January, 2008);  
<http://www.geocities.jp/hjrfq930/Papers/paperr/paperr.html>

[Kozima 2008c] H. Kozima, “Physics of the Cold Fusion Phenomenon,” *Proc. ICCF13*, pp. 690 – 703 (2008). ISBN 978-5-93271-428-7. And also *Reports of CFRL* **11-4**, pp. 1 – 21 (January, 2011);  
<http://www.geocities.jp/hjrfq930/Papers/paperr/paperr.html>

[Kozima 2010a] H. Kozima, “Neutron Emission in the Cold Fusion Phenomenon,” *Proc. JCF11*, pp. 76 – 82 (2010). ISSN 2187-2260: <http://jcf11-proceedings.pdf>  
 And also *Reports of CFRL (Cold Fusion Research Laboratory)* **11-3**, 1 – 12 (January, 2011); <http://www.geocities.jp/hjrfq930/Papers/paperr/paperr.html>

[Kozima 2010b] H. Kozima, “Localization of Nuclear Reactions in the Cold Fusion Phenomenon,” *Proc. JCF11*, pp. 59 – 69 (2010). ISSN 2187-2260.  
<http://jcf11-proceedings.pdf>  
 And also *Reports of CFRL (Cold Fusion Research Laboratory)* **11-2**, 1 – 20 (January, 2011); <http://www.geocities.jp/hjrfq930/Papers/paperr/paperr.html>

[Kozima 2013] H. Kozima, “Cold Fusion Phenomenon in Open, Nonequilibrium, Multi-component Systems – Self-organization of Optimum Structure,” *Proc. JCF13*, 13-19, pp. 134 – 157 (2013), ISSN 2187-2260, and is posted at JCF website:  
<http://jcf13-proceedings.pdf>

The paper is also published as *Reports of CFRL* **13-3**, pp. 1 – 24 (2013) and posted at CFRL website: <http://www.geocities.jp/hjrfq930/Papers/paperr/paperr.html>

[Kozima 2014a] H. Kozima and K. Kaki, “Atomic Nucleus and Neutron — Nuclear Physics Revisited with the Viewpoint of the Cold Fusion Phenomenon,” *Proc. JCF14*, **14-6**, pp. 47 – 76 (2014). ISSN 2187-2260: <http://jcf14-proceedings.pdf>  
 And also *Reports of CFRL (Cold Fusion Research Laboratory)* **14-1**, 1 – 31 (March, 2014); <http://www.geocities.jp/hjrfq930/Papers/paperr/paperr.html>

[Kozima 2014b] H. Kozima, “Nuclear Transmutations (NTs) in Cold Fusion

Phenomenon (CFP) and Nuclear Physics,” *Proc. JCF14*, **14-15**, pp. 168 – 202 (2014).

ISSN 2187-2260: <http://jcfrs.org/file/jcf14-proceedings.pdf>

And also *Reports of CFRL* (Cold Fusion Research Laboratory) **14-3**, 1 – 37 (March, 2014); <http://www.geocities.jp/hjrfq930/Papers/paperr/paperr.html>

[Negele 1973] J.W. Negele and D. Vautherin, “Neutron Star Matter at Sub-nuclear Densities,” *Nuclear Physics*, **A207**, 298 - 320 (1973).

[Rundle 1947] R.E. Rundle, “The Structure of Uranium Hydride and Deuteride,” United State Atomic Commission MDDC-865, pp. 1 - 9 (1947).